JACS
JOURNAL OF THE AMERICAN CHEMICAL SOCIETY

Article

pubs.acs.org/JACS

Photoligation of an Amphiphilic Polymer with Mixed Coordination Provides Compact and Reactive Quantum Dots

Wentao Wang,[†] Anshika Kapur,[†] Xin Ji,[†] Malak Safi,[†] Goutam Palui,[†] Valle Palomo,[‡] Philip E. Dawson,[‡] and Hedi Mattoussi*,[†]

[†]Department of Chemistry and Biochemistry, Florida State University, Tallahassee, Florida 32306, United States

[‡]Department of Chemistry and Department of Cell Biology, The Scripps Research Institute, 10550 N. Torrey Pines Road, La Jolla, California 92037, United States

Supporting Information

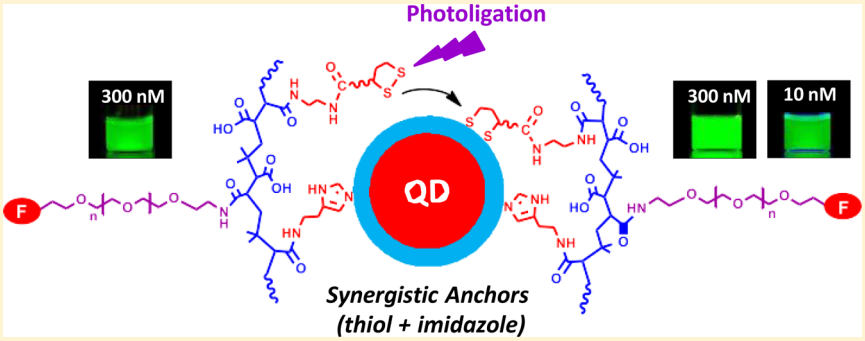

ABSTRACT: We introduce a new set of multicoordinating polymers as ligands that combine two distinct metal-chelating groups, lipoic acid and imidazole, for the surface functionalization of QDs. These ligands combine the benefits of thiol and imidazole coordination to reduce issues of thiol oxidation and weak binding affinity of imidazole. The ligand design relies on the introduction of controllable numbers of lipoic acid and histamine anchors, along with hydrophilic moieties and reactive functionalities, onto a poly(isobutylene-*alt*-maleic anhydride) chain via a one-step nucleophilic addition reaction. We further demonstrate that this design is fully compatible with a novel and mild photoligation strategy to promote the in situ ligand exchange and phase transfer of hydrophobic QDs to aqueous media under borohydride-free conditions. Ligation with these polymers provides highly fluorescent QDs that exhibit great long-term colloidal stability over a wide range of conditions, including a broad pH range (3−13), storage at nanomolar concentration, under ambient conditions, in 100% growth media, and in the presence of competing agents with strong reducing property. We further show that incorporating reactive groups in the ligands permits covalent conjugation of fluorescent dye and redox-active dopamine to the QDs, producing fluorescent platforms where emission is controlled/tuned by Förster Resonance Energy Transfer (FRET) or pH-dependent charge transfer (CT) interactions. Finally, the polymer-coated QDs have been coupled to cell-penetrating peptides to facilitate intracellular uptake, while subsequent cytotoxicity tests show no apparent decrease in cell viability.

INTRODUCTION

Fluorescent semiconductor nanocrystals (quantum dots, QDs) combine several unique optical and spectroscopic properties that can be tuned via size and/or composition.[1−6] For instance, core−shell QDs, such as those made of ZnS-overcoated CdSe nanocrystals, exhibit narrow tunable emission throughout the visible spectrum, combined with high quantum yield and a remarkable resistance to chemical degradation.[7−12] These unique features have made them greatly appealing for use as in vivo and in vitro fluorescent probes in a variety of biomedical applications; these include cellular labeling, deep-tissue imaging, biochemical sensing, and drug delivery vehicles.[11,13−27]

Highly fluorescent QDs with good control over size and crystallinity are mostly grown via reduction of organometallic precursors at high temperature and in the presence of hydrophobic coordinating ligands.[3,4,7−10] This growth route yields nanocrystals that are only dispersible in organic solvents. A key requirement for a successful integration of these materials into biology is access to an effective and reproducible surface-modification strategy.[23,28−32] Cap exchange with bifunctional coordinating ligands has been used by several groups to promote the dispersion of various inorganic nanocrystals in buffer media. This strategy relies on the competitive removal of the hydrophobic capping molecules and their replacement with hydrophilic metal-coordinating ligands.[23] The strength of the ligand coordination onto the nanocrystal surface along with a strong affinity of the hydrophilic modules to buffer media

Received: January 20, 2015
Published: March 22, 2015

DOI: 10.1021/jacs.5b00671
J. Am. Chem. Soc. 2015, 137, 5438−5451

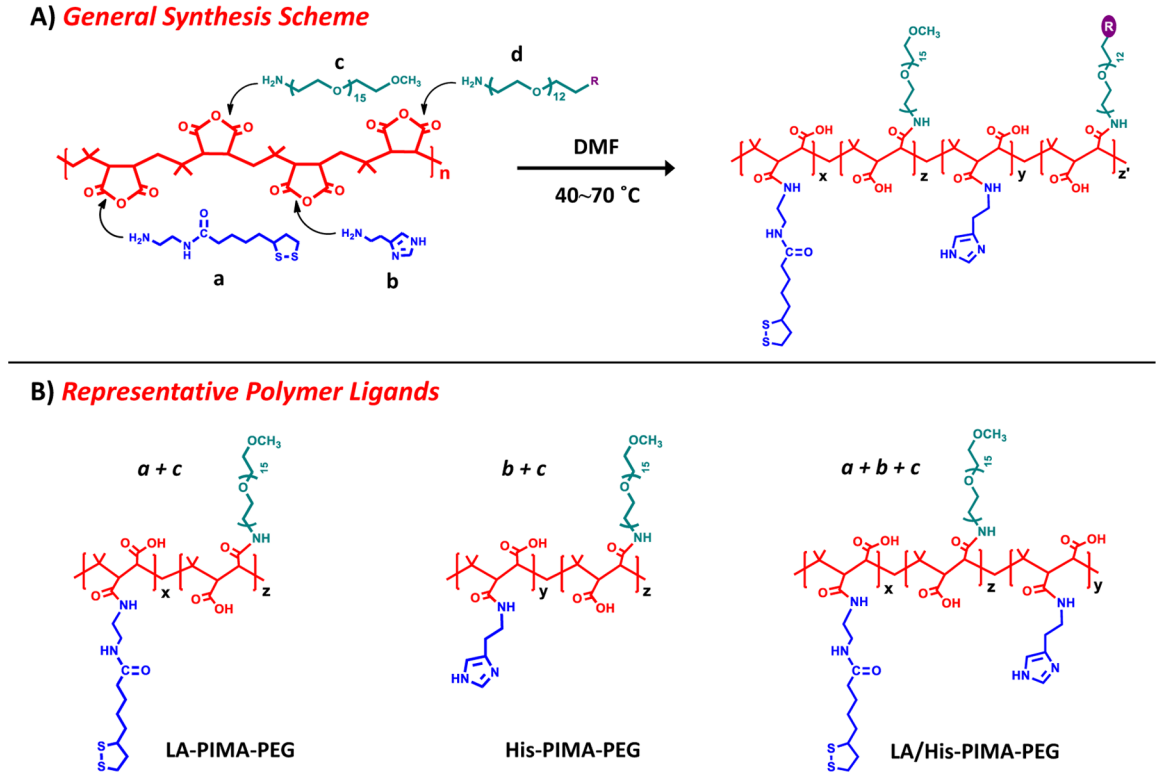

Figure 1. (A) Schematic representation of the one-step nucleophilic addition reaction used to prepare the various multidentate lipoic acid and histamine-modified polymers based on the PIMA motif. (B) Structures of a few representative ligands are shown: LA−PIMA−PEG, His−PIMA−PEG, and LA/His−PIMA−PEG.

ultimately control the long-term colloidal stability of the QDs in biological environments.

Ligands presenting multiple thiol groups, such as derivates of dihydrolipoic acid (DHLA), greatly enhance the QD colloidal stability in various biological conditions, compared with those presenting monothiol or other weakly coordinating groups.[33−40] The multicoordination interactions between the QD and multidentate ligands decrease the ligand desorption rate from the nanocrystal surfaces, substantially improving the colloidal stability of the QDs in biological media. Nevertheless, thiol-terminated ligands tend to negatively affect the photoluminescence properties of the hydrophilic QDs.[41] Moreover, under ambient conditions (e.g., room temperature and light exposure) most thiol-based ligands can be affected by photooxidation during extended storage time, which causes ligand desorption from the QD surface.[28,42,43] This problem becomes more serious at very low concentrations, since the dynamic equilibrium of coordination favors higher dissociation rates. To address some of these limitations, polymer ligands presenting multiple imidazole (or pyridine) groups have been developed as an alternative to thiol groups for coordination on the nanocrystal.[42,44−47] Imidazole is not affected by this oxidation problem and has been found to potentially enhance the QD emission.[48] However, imidazole and pyridine exhibit weaker coordination affinity to the nanocrystal surfaces than thiols. For instance, histidine-coated QDs can be easily exchanged by thiol-terminated ligands.[49] Furthermore, imidazole-based polymer ligands provide hydrophilic QDs that exhibit colloidal stability only in weakly acidic to alkaline pH since the imidazole groups tend to be protonated under acidic conditions (pH < 6).[44,50] This limits their use for common and newer promising conjugation techniques (e.g., EDC coupling and hydrazide reaction are most efficient at pH 4−6).[51]

Building on those observations, we hypothesized that combining the two metal-chelating groups, thiol (or lipoic acid, LA) and imidazole, within the same polymer structure could enhance the overall ligand-to-QD affinity and maintain high quantum yield, while reducing issues associated with oxidation of the thiol and weak coordination of the imidazole. In the present study, we introduce a new set of multicoordinating and multifunctional polymer ligands that can tightly ligate onto the surface of QDs. Our ligand design relies on the use of a simple one-step nucleophilic addition reaction between distinct amine-modified molecules and maleic anhydride groups to introduce large and controllable numbers of lipoic acid and imidazole groups along the same polymer backbone. More precisely, amine-terminated lipoic acid, histamine, and poly(ethylene glycol) (PEG) moieties are reacted with poly(isobutylene-*alt*-maleic anhydride) (PIMA) in an organic medium to provide a polymer ligand containing tunable numbers of LAs, imidazoles, and PEG moieties. Furthermore, we demonstrate that this ligand design is fully compatible with a novel and mild photoligation strategy to promote the in situ ligand exchange and phase transfer of QDs to aqueous media under borohydride-free conditions. Ligation of the QDs with these polymers combines the benefits of thiol and imidazole coordination, and provides highly fluorescent QDs that exhibit great long-term colloidal stability over a wide range of conditions, including storage at nanomolar concentration, under ambient conditions, in 100% growth media and in the presence of competing reducing agents. In addition, this strategy provides compact QDs that are suitable for use in energy and charge transfer interactions. We show that

DOI: 10.1021/jacs.5b00671
J. Am. Chem. Soc. 2015, 137, 5438−5451

Table 1. Summary of the Prepared Ligands, along with the Nominal and Experimentally Estimated Numbers of Coordinating Groups and PEG Moieties per PIMA Chain for Each Compound

ligand	(molar fractions)	nominal numbers per chain[a]				experimental numbers per chain[b]		
LA–PIMA–PEG	(x:z = 30:70)	LA: 12	PEG: 27			LA: ∼13	PEG: ∼27	
His–PIMA–PEG	(y:z = 30:70)	His: 12	PEG: 27			His: ∼10	PEG: ∼27	
His–PIMA–PEG	(y:z = 50:50)	His: 20	PEG: 20			His: ∼17	PEG: ∼19	
LA/His–PIMA–PEG	(x:y:z = 20:30:50)	LA: 8	His: 12	PEG: 20		LA: ∼10	His: ∼12	PEG: ∼18
LA/His–PIMA–PEG–R	(x:y:z:z′ = 20:30:45:5)	LA: 8	His: 12	PEG: 18	R: 2			

[a]The reported values for the various moieties were obtained from the starting molar concentrations of the amine-modified molecules (e.g., lipoic acid–amine (x), histamine (y), PEG–amine (z), and R–PEG–amine (z′)) in comparison to that of the maleic anhydride groups of the PIMA. [b]The values were obtained by comparing the ^{1}H NMR peak integration of the LA ($\delta \sim 2.1$ ppm), His ($\delta \sim 6.8$ ppm), and PEG ($\delta \sim 3.2$ ppm) to the methyl groups of PIMA (∼234 H, $\delta \sim 0.8$–1.0 ppm). The corresponding ^{1}H NMR spectra are provided in the Supporting Information (Figures S2–S4).

incorporating amine reactive groups in the polymer ligand permits covalent conjugation of fluorescent dye and redox-active dopamine to the QDs, producing fluorescent platforms where emission can be controlled/tuned by Förster Resonance Energy Transfer (FRET) or via pH-dependent charge transfer (CT) interactions. We also show that these polymer-coated QDs can be easily coupled to cell-penetrating peptides (CPP), facilitating intracellular uptake, while eliciting little to no change in the cell viability.

RESULTS AND DISCUSSION

Ligand Design. The polymer ligands developed in this work are prepared via one-step nucleophilic addition reaction between PIMA and amine-modified molecules, namely lipoic acid–amine, histamine, and PEG–amine. This synthetic scheme has a few unique features. The reaction can be carried out in the absence of coupling reagents or excess precursors, which simplifies purification of the final product(s). The presence of several maleic anhydrides (∼39) along the backbone allows for the simultaneous insertion of a large but controllable number of distinct and complementary functionalities within the same ligand: lipoic acid and/or imidazole anchoring groups for strong coordination on the QDs, PEG moieties for water solubilization and biocompatibility, and reactive functionalities for targeted conjugation to biomolecules. Additionally, the presence of dimethyl groups between adjacent anhydride rings combined with the cis–trans configuration of the polymer backbone reduces the steric constraints and enhances reactivity, which allows high degrees of substitutions during the addition reaction.

We should emphasize that similar polymer precursors have been used by other groups to design amphiphilic block copolymers to encapsulate QDs and iron oxide nanoparticles within micelle-like structures.[52−57] However, the present ligand design and the surface functionalization strategy are drastically different from the one relying on encapsulation within block copolymers. Our approach requires the removal of the native cap and involves direct coordination of the new ligands on the QD surfaces. The presence of several metal chelating groups and PEG moieties within the same ligand respectively promote strong coordination on the nanocrystal surface and water solubilization. The multidentate interactions of the polymer ligand yield compact coating, which decreases the hydrodynamic size (compared to encapsulation) and substantially improves the colloidal stability of the final nanocrystals, while allowing surface reactivity (see below).

The synthesis starts with commercially available PIMA (MW, 6000 g/mol; ∼39 maleic anhydride monomers per chain). Figure 1 shows a schematic representation of the general synthetic route used to prepare lipoic acid and histamine-based ligands. The nucleophilic addition reaction yields lateral distinct functionalities attached to the chain via amide bonds; it also frees several carboxylic acid groups along the backbone (as many as the number of maleic anhydrides), which provide additional hydrophilicity and potential reactive groups for bioconjugation. The architecture of the final ligand can be optimized by controlling the molar ratio of each amine-modified moiety with respect to the maleic anhydride groups in the PIMA chain. Employing this platform, we have designed four sets of polymer ligands: LA–PIMA–PEG, His–PIMA–PEG, LA/His–PIMA–PEG, and LA/His–PIMA–PEG–R, where R designates a reactive group, such as amine, azide, and biotin; a summary list of the ligands prepared in this study is provided in Table 1.

The first set, LA–PIMA–PEG, is prepared by reacting PIMA with a mixture of 30% lipoic acid–amine and 70% methoxy–PEG–amine. Here, the molar fraction of maleic anhydrides reacted with LA–NH_2 is maintained at 30% or smaller to avoid issues of insolubility encountered in ref 35 (with poly(acrylic acid) precursor), although higher fractions of lipoic acid can be introduced using the current synthetic route. The second set is made of His–PIMA–PEG. The synthesis is similar to that of LA–PIMA–PEG, but the lipoic acid–amine is replaced with histamine. The molar ratio of histamine:PEG–amine could be adjusted from 30:70 to 50:50, allowing a side-by-side comparison with other ligands. In this work, we focus on the ligand prepared with histamine:PEG–amine molar ratio of 50:50. The third set is made of LA/His–PIMA–PEG, which contains a stoichiometric mixture of 20% LA, 30% histamine, and 50% methoxy–PEG per chain. The last set, LA/His–PIMA–PEG–R, is made of a stoichiometric mixture of LA (20%), histamine (30%), methoxy–PEG (45%), and reactive PEG moieties (5%). This is achieved by replacing 5% of methoxy–PEG–amine with R–PEG–amine during the reaction. Here we show one example of amine functionalized polymers, but other reactive ligands can be easily obtained by changing the type of reactive group used (e.g., starting with azide–PEG–amine or biotin–PEG–amine).[58,59] In particular, if a mixture of different R–PEG–amine moieties (e.g., azide(R_1)–PEG–amine along with biotin(R_2)–PEG–amine) is used to prepare the amphiphilic polymer, this can yield hydrophilic QDs that are ideally adapted for orthogonal coupling to target molecules. Additional details about the ligand synthesis and ^{1}H NMR characterization are provided in the Experimental Section and Supporting Information (SI). Overall, the data shown in Table 1 indicate that the molar

DOI: 10.1021/jacs.5b00671
J. Am. Chem. Soc. 2015, 137, 5438−5451

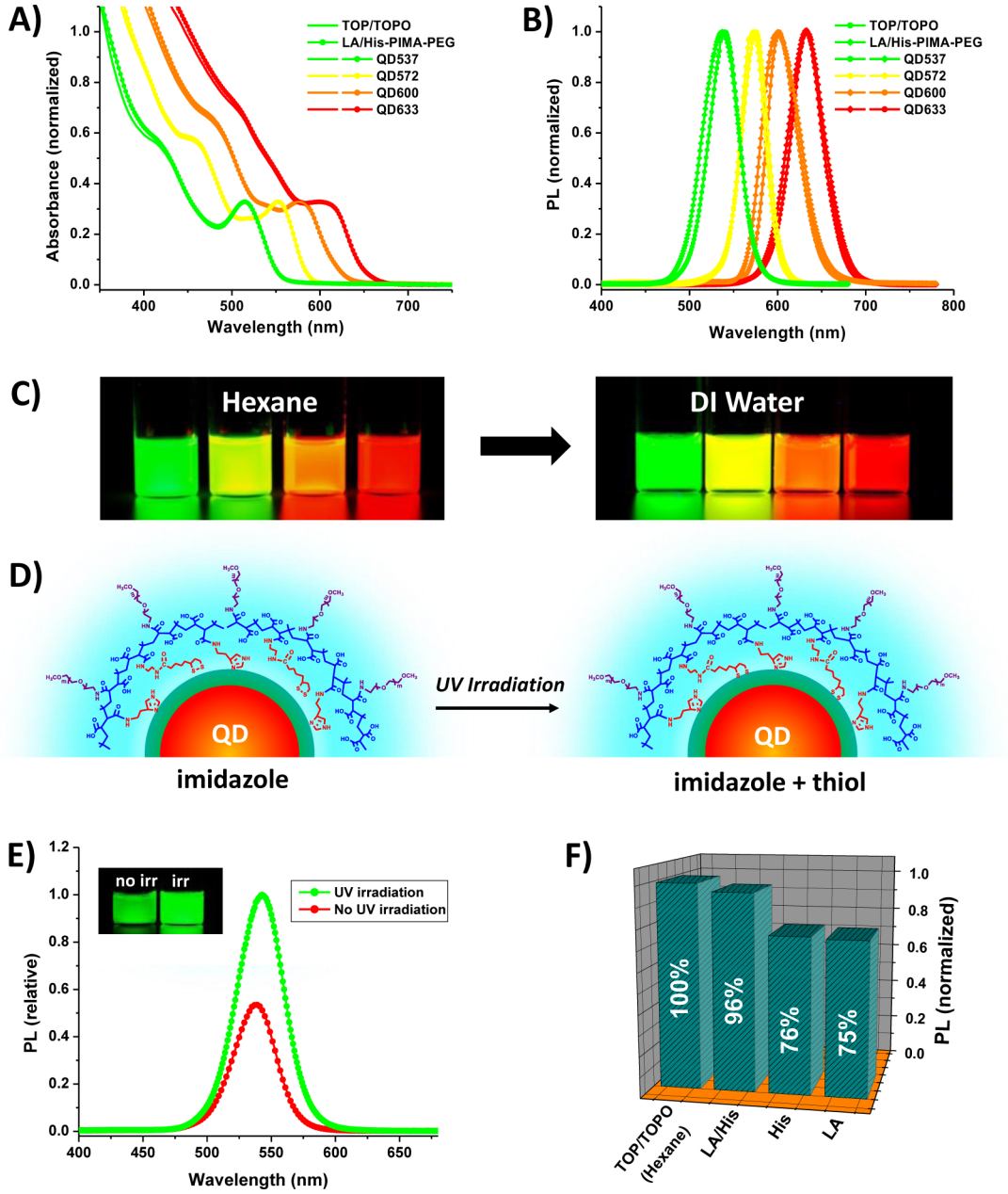

Figure 2. (A) Normalized absorbance and (B) emission spectra of four representative QDs emitting at 537, 572, 600, and 633 nm, before and after photoligation with LA/His–PIMA–PEG ligands. (C) Fluorescence images of four sets of QDs capped with TOP/TOPO in hexane and photoligated with LA/His–PIMA–PEG in water. (D) Schematic depiction of the selective binding of LA anchors on the QDs before and after UV irradiation. (E) Plot of the PL intensity for QDs ligated with LA/His–PIMA–PEG before and after UV irradiation, showing ~2× enhancement in the PL following exposure to UV light; the corresponding fluorescence images are shown in the inset. (F) Relative PL intensities collected from the three QD samples dispersed in buffer (pH 7.5) with respect to that measured for the native TOP/TOPO–QDs in hexane. The optical densities for all samples are maintained the same, with QD concentration ~0.1 μM.

fractions of the various moieties per PIMA chain (i.e., stoichiometry), extracted from the ^{1}H NMR spectra, are consistent with the nominal values of the starting amine-modified molecules used during the addition reaction. For instance, for LA/His–PIMA–PEG we measured multiplet peaks at ~1.1–2.4 ppm and ~3.1 ppm characteristic of the lipoic acid protons, two peaks at ~6.8 and ~7.6 ppm ascribed to the protons of the imidazole ring, along with a strong peak at ~3.5 ppm and a sharp peak at ~3.2 ppm attributed to the PEG and terminal methoxy protons, respectively. A broad peak at ~0.9 ppm ascribed to the methyl protons of the polymer backbone was also measured. The degree of grafting was estimated by comparing the integration ratio of ^{1}H NMR peaks of LA (2 H, δ ~2.1 ppm), His (1 H, δ ~6.8 ppm), methoxy group (3 H, δ ~3.2 ppm) to the two methyl repeat units in a PIMA chain (~234 H, δ ~0.9 ppm). We deduced that ~10 lipoic acid groups (21.0 H), ~12 histamines (12.4 H), and ~18 methoxy groups (54.0 H, i.e., 18 PEG moieties) were introduced per chain. Additional details on the NMR data and stoichiometry of the ligand structures are provided in the SI (e.g., see Figures S2–S4).

Ligand Exchange and Phase Transfer. Ligand exchange of CdSe–ZnS QDs with LA-containing ligands is carried out under borohydride-free conditions using a novel and mild

DOI: 10.1021/jacs.5b00671
J. Am. Chem. Soc. 2015, 137, 5438–5451

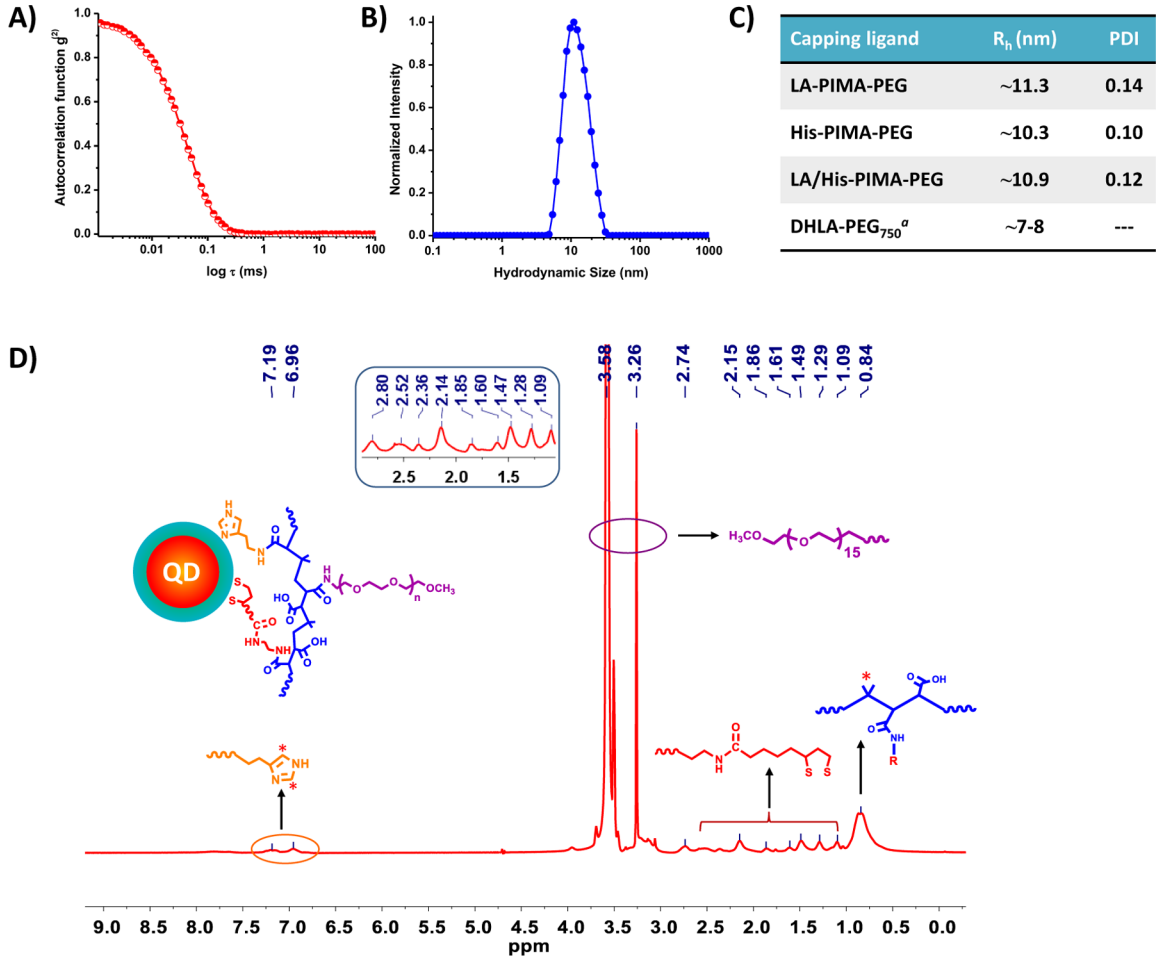

Capping ligand	R_h (nm)	PDI
LA-PIMA-PEG	~11.3	0.14
His-PIMA-PEG	~10.3	0.10
LA/His-PIMA-PEG	~10.9	0.12
DHLA-PEG$_{750}$[a]	~7-8	---

Figure 3. (A) Representative plot of the autocorrelation function, ($g^{(2)}$) vs. log lag time (τ), collected from a dispersion of QDs (emission at 537 nm) photoligated with LA/His−PIMA−PEG. (B) Histograms showing the distribution of the intensity vs hydrodynamic radius, extracted from the Laplace transform of the autocorrelation function shown in (A). (C) Hydrodynamic radius (R_H) values and polydispersity index (PDI) measured for 537-nm-emitting QDs ligated with LA−PIMA−PEG, His−PIMA−PEG, LA/His−PIMA−PEG and DHLA−PEG$_{750}$ (control). [a]The R_H value is reproduced from ref 66. (D) ^{1}H NMR spectrum collected from QDs ligated with LA/His−PIMA−PEG dispersed in D_2O.

photoligation strategy.[60] We have previously shown that such strategy is applicable to an array of LA-based small molecules, including LA−PEG−OMe, LA−PEG−COOH/NH$_2$, and bis-(LA)−zwitterion.[34,60] Here, we expand this strategy to polymer ligands, namely LA−PIMA−PEG, LA/His−PIMA−PEG, and LA/His−PIMA−PEG−NH$_2$.

The effectiveness of the photoligation strategy applied to LA-based ligands stems from the photochemical sensitivity of the strained dithiolane ring to UV excitation. Indeed, LA exhibits a well-defined absorption peak at ~340 nm. This absorption peak continuously decreases with time to nearly background level after ~20−30 min of UV irradiation at 350 nm; such change has been attributed to the photochemical transformation of the dithiolane to several products including dithiol groups and dithiol radicals.[60,61] Here too, we find that UV irradiation of LA−PIMA−PEG yields similar change in the optical feature of the dithiolane ring, though this change is less pronounced due to rather strong background contribution from the polymer to the absorption spectrum (see SI Figure S5). In the case of LA/His−PIMA−PEG, a slightly shorter irradiation time (~10 min) was needed, presumably due to the smaller number of lipoic acid groups per PIMA chain compared with LA−PIMA−PEG. It is worth noting that following irradiation of the LA/His−PIMA−PEG ligand, the measured absorption profile is essentially identical to that collected from pure His−PIMA−PEG, indicating that the imidazole groups do not exhibit a photochemical response. We further verified that the absorption feature and ^{1}H NMR characteristic peaks of His−PIMA−PEG are not altered by UV irradiation (see SI Figure S5 for more details).

The photoligation of QDs with LA−PIMA−PEG was performed using one phase configuration, where hydrophobic QDs and ligands were dispersed in THF followed by the addition of a small amount of tetramethylammonium hydroxide catalyst predissolved in methanol. The mixture was irradiated for 20 min, while stirring, using a UV reactor, followed by precipitation with excess hexane. After evaporation of the residual solvent under vacuum, the QDs were readily dispersed in DI water. For LA/His−PIMA−PEG or LA/His−PIMA−PEG−R, ligand exchange was carried out using a slightly modified procedure. The mixture of hydrophobic QDs and ligands in THF was first stirred for 2 h prior to UV irradiation. This allowed for imidazole coordination onto the QD surfaces. In this case the photoirradiation can be applied to the LA groups along the ligated polymer in either organic solvent, or even aqueous media (if the QDs were transferred to water after 2-h reaction in THF). Cap exchange with His−PIMA−PEG was carried out by mixing the hydrophobic QDs and His−

DOI: 10.1021/jacs.5b00671
J. Am. Chem. Soc. 2015, 137, 5438−5451

PIMA−PEG ligands in THF and stirring the mixture for 2 h at 40 °C, followed by purification. These procedures yielded QDs that were readily dispersed in water.

Characterization of the Hydrophilic QDs. The hydrophilic QD dispersions have been characterized using three complementary analytical techniques: (1) absorption and fluorescence spectroscopy, (2) dynamic light scattering, and (3) ^{1}H NMR spectroscopy. ^{1}H NMR was further utilized to estimate the surface ligand density.

1. Optical Characterization. Figure 2A and B show absorption and emission spectra of 4 representative sets of QDs emitting at 537, 572, 600, and 633 nm, before and after photoligation with LA/His−PIMA−PEG ligands. The spectral properties of the QDs capped with LA/His−PIMA−PEG are essentially identical to those measured for hydrophobic nanocrystals dispersed in hexane. Similar data were collected for QDs ligated with His−PIMA−PEG and LA−PIMA−PEG (see SI Figure S6). However, a slight red shift (∼1−5 nm) in absorption and emission peaks was measured for QDs photoligated with LA−PIMA−PEG, a result consistent with previous findings combining photoligation and LA−PEG-based ligands.[60] Overall, the ligand exchange was rapid and yielded aqueous QD dispersions that exhibited strong fluorescence under UV light, as shown in Figure 2C.

Influence of the Photoligation on the QD Emission Properties. We investigated the effects of combining mixed anchors (LA and His) with photoligation on the emission properties of the resulting water-soluble QDs. For this we conducted ligand exchange of TOP/TOPO−QDs with LA/His−PIMA−PEG in two steps. First, ligand exchange was carried out without involving UV-irradiation and the PL spectrum was collected. Here, we anticipate that only the imidazole groups coordinate on the QD surface, leaving the LA groups (in the form of dithiolanes) unattached, because the oxidized groups do not coordinate on the QD surface (see illustration in Figure 2D).[33] In the next step UV irradiation was applied to the QD dispersion in buffer for 10 min, to allow ligation of the photochemically transformed dithiol groups onto the QD surfaces. Figure 2E shows a side-by-side comparison of the fluorescence images and PL spectra collected from the same sample before and after UV irradiation. Clearly, dispersions of photoligated QDs exhibit a stronger fluorescence, i.e., an enhancement of ∼2 is measured. This brightening may be attributed to a combination of the following: (1) the synergistic effect of two anchoring groups (instead of one) which reduces the ligand desorption and improves the colloidal stability, and (2) the benefit of imidazole coordination on the QD exciton radiative recombination as previously reported.[48] Additional contribution may emanate from UV-promoted photoannealing of QDs, which can lead to enhancement of the photoluminescence by reducing the number of surface trap states.[42,62−65] Indeed, such photoinduced enhancement in the PL was also observed for His−PIMA−PEG QDs following irradiation for 10 min in the UV reactor, though the measured enhancement was smaller (see SI Figure S7).

We finally compared the photoluminescence intensities measured from dispersions of QDs ligated with different polymer ligands in buffer (pH 7.5) with that measured from TOP/TOPO−QDs in hexane; the optical densities were maintained identical for all samples. We found that QDs photoligated with LA/His−PIMA−PEG yielded the highest PL, with intensity comparable to that measured from a dispersion of TOP/TOPO−QDs. In comparison, the PL measured from dispersions of QDs ligated with LA−PIMA−PEG or His−PIMA−PEG were slightly lower, with respective intensities equal to ∼75% and 76% of that measured for TOP/TOPO−QDs in hexane (see Figure 2F).

2. Dynamic Light Scattering Measurements. The hydrodynamic sizes were obtained from multiangle dynamic light scattering (DLS) measurements applied to three sets of QD dispersions (emission at 537 nm) ligated with LA−PIMA−PEG, His−PIMA−PEG, and LA/His−PIMA−PEG, dispersed in DI water (pH ∼6.5). Figure 3A shows a representative plot of the intensity autocorrelation function, $g^{(2)}$ versus lag time, collected from the LA/His−PIMA−PEG−QD dispersions in water at a scattering angle $\theta = 90°$. Additional plots for $g^{(2)}$, collected using various θ values (ranging from 60° to 150°), consistently showed that faster decay rates were measured for higher scattering angles as expected (data not shown). Furthermore, a linear dependence of the decay rate versus the square of the scattering wavevector was extracted from the data.[66] Similar data were collected for the other two sets of QD dispersions. These profiles exhibit faster decays in comparison to those measured for iron oxide and gold nanoparticles,[59,67] indicating faster diffusion coefficients for smaller size nanocrystals. The corresponding histograms for the intensity vs hydrodynamic size, extracted from the Laplace transform of the autocorrelation function, along with the polydispersity index (PDI) values, are shown in Figure 3. The hydrodynamic radii extracted from these measurements are ∼10.9 nm for LA/His−PIMA−PEG−QDs, ∼10.3 nm for His−PIMA−PEG−QDs, and ∼11.3 nm for LA−PIMA−PEG−QDs (Figure 3C). These are only ∼2−3 nm larger than what was reported for DHLA−PEG_{750}−OCH_3-capped QDs.[66] This compact size reflects the nature of the multicoordinating ligands, yielding homogeneous QDs with a thin polymer coating.

3. ^{1}H NMR Characterization. The dispersion of QDs ligated with LA/His−PIMA−PEG (in D_2O) were further characterized using pulsed-field gradient-based water suppression ^{1}H NMR spectroscopy. Figure 3D shows the ^{1}H NMR spectrum collected from a dispersion of QDs photoligated with LA/His−PIMA−PEG; this spectrum is essentially identical to the one collected from the ligand alone (shown in SI Figure S4). However, the two resonances at 6.96 and 7.19 ppm, characteristic of protons in the imidazole ring, are weaker and slightly shifted with respect to the peaks measured for the ligand alone. Such shift is attributed to binding of the imidazole to the QD and a change in its environment. The spectrum in Figure 3D also shows that the NMR signatures of the TOP/TOPO/HPA measured for the native hydrophobic QDs (e.g., peaks at 0.82 and 1.23 ppm shown in SI Figure S8) are conspicuously absent. These results combined clearly indicate that cap exchange of the QDs and their transfer to buffer media involved removal of the TOP/TOPO/HPA and ligation of LA/His−PIMA−PEG onto the QD surfaces, driven by coordination of imidazole and photochemically modified LA groups.

We further used ^{1}H NMR measurements to extract an estimate for the average number of LA/His−PIMA−PEG per QD, by comparing the molar concentrations of the ligand and QDs following phase transfer and removal of excess unbound ligands. The molar amount of the LA/His−PIMA−PEG was estimated by comparing the integrations of the methyl-protons on the PIMA backbone and the α-proton of the pyridine standard, while the concentration of QDs was estimated from the optical absorption at 350 nm. Such analysis indicates that for ∼3-nm radius QDs (core-plus-shell size extracted from

DOI: 10.1021/jacs.5b00671
J. Am. Chem. Soc. 2015, 137, 5438−5451

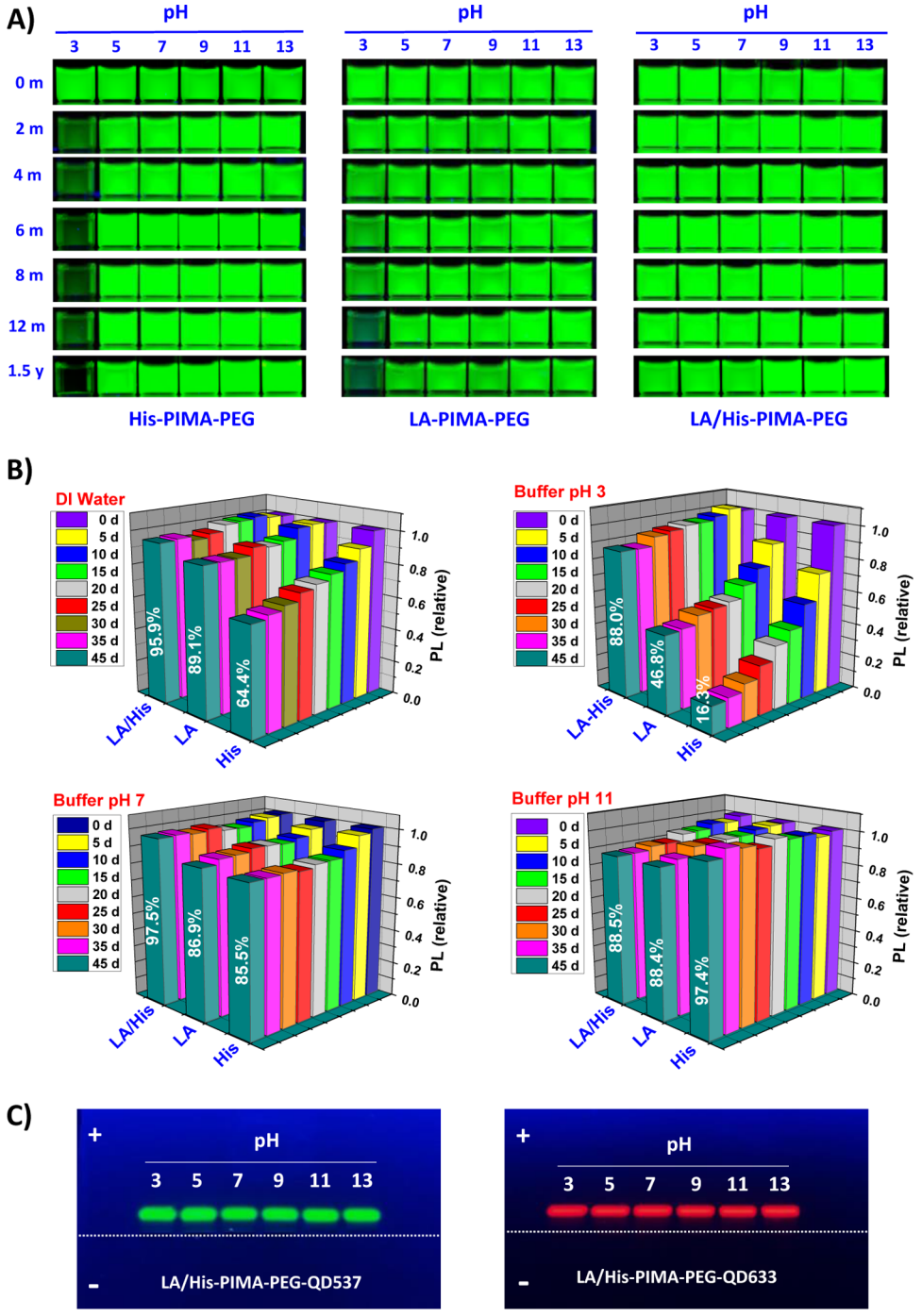

Figure 4. (A) Colloidal stability tests of QDs ligated with His−PIMA−PEG, LA−PIMA−PEG, and LA/His−PIMA−PEG dispersed in phosphate buffer (20 mM) from pH 3 to 13. The concentration of QDs is ∼0.5 μM. (B) Time progression of the fluorescence intensities of QDs (∼0.3 μM) capped with His−PIMA−PEG, LA−PIMA−PEG, and LA/His−PIMA−PEG dispersed in DI water and in different pH buffers. The intensity is normalized with respect to the value measured at 0 day. (C) Agarose gel electrophoresis images of green- and red-emitting QDs ligated with LA/His−PIMA−PEG dispersed in buffers with different pH from 3 to 13. The concentration of QDs is ∼0.5 μM. The dashed line indicates the location of the wells. Gel running conditions are provided in the SI.

TEM and small-angle X-ray scattering),[3,68] with emission peak at 537 nm, there are about 14.5 polymer ligands, which corresponds to ∼290 anchors (histamine plus DHLA) and ∼261 PEG moieties per nanocrystal. When such analysis is applied to QDs ligated with LA/His−PIMA−PEG−NH_2 (5% amine), we roughly estimate that there are ∼28 amine groups per nanocrystal. The ^{1}H NMR spectrum of hydrophilic QDs mixed with pyridine standard is provided in SI Figure S9. Though these values constitute only approximate estimates for the number of ligands, the resulting number of PEG moieties is comparable to those reported for LA−PEG-coated Au nanoparticles.[69]

Colloidal Stability Tests. We have tested the stability of three representative sets of QDs, one set photoligated with LA/His−PIMA−PEG, one photoligated with LA−PIMA−PEG, and one capped with His−PIMA−PEG. Tests focused on

DOI: 10.1021/jacs.5b00671
J. Am. Chem. Soc. 2015, 137, 5438−5451

several biologically relevant conditions, including (1) the pH 3−13 range, (2) in high ionic strength buffer (1 M NaCl), (3) in the presence of competing reducing molecules (0.5 M dithiothreitol, DTT), (4) in 100% cell growth media (RPMI-1640 Medium), and (5) storage at low concentration (10 nM) at 4 °C in the dark and under room temperature with light exposure conditions.

Figure 4A shows side-by-side fluorescence images acquired from three sets of green-emitting QD dispersions (0.5 μM) over the pH range from 3 to 13, as prepared and after different storage periods extending to 1.5 years. Data show that QDs photoligated with LA/His−PIMA−PEG remained stable over the full pH range, with no sign of aggregate build up or loss in fluorescence. In comparison, the dispersions of QDs either ligand exchanged with His−PIMA−PEG or photoligated with LA−PIMA−PEG were stable over the pH range 5−13. However, dispersions at pH 3, though remaining colloidally stable, exhibited a progressive and substantial loss in emission after ∼8 months for LA−PIMA−PEG−QDs; a more pronounced loss was observed after ∼1 month for His−PIMA−PEG−QDs. The images in Figure 4A also show that dispersions of LA−PIMA−PEG−QDs were less fluorescent than the other two samples over the storage period, a property attributed to the nature of the thiol-coordination.[41]

Figure 4B shows a side-by-side comparison of the PL intensity progression with storage time for QD dispersions (0.3 μM) in DI water (pH ∼6.5), and in buffers at pH 3, pH 7, and pH 11. The data indicate that under neutral and basic conditions, the PL intensity remained essentially constant. In comparison, only dispersions of LA/His−PIMA−PEG−QDs maintained both colloidal stability and high emission at pH 3 over the full test period. The PL and colloidal stability of His−PIMA−PEG−QDs and LA−PIMA−PEG−QDs was weaker, though losses were much more pronounced for His−PIMA−PEG−QDs. For example, after 45 days of storage at pH 3, the PL intensities of the LA−PIMA−PEG−QDs and His−PIMA−PEG−QDs respectively decayed to ∼47% and ∼16% (compared to freshly prepared samples), but dispersions stayed homogeneous. The colloidal stability of LA/His−PIMA−PEG−QDs at different pH was further verified using 0.6% agarose gel electrophoresis measurements. As shown in Figure 4C, the fluorescent bands at the various pHs, visualized using the fluorescence signal of the QDs, consistently show that the QDs migrate toward the anode with similar mobility shift and very narrow bands at all pHs, confirming the uniform distribution in size and colloidal stability. In addition, the single mobility shifts measured for all samples reflect a homogeneous surface charge on the QDs attributed to the carboxylic groups on the polymer ligand.

Results of the colloidal stability tests applied to the polymer-ligated QDs in high ionic strength solutions and in the presence of strong reducing agent (dithiothreitol, DTT) are summarized in Figure 5A and B. All three sets of QD dispersions stayed stable and aggregate-free for at least 12 months of storage in the presence of 1 M NaCl, though a slight loss in the PL signal was observed for nanocrystals capped with His−PIMA−PEG after 8 months. Figure 5B shows that dispersions of QDs ligated with the three sets of polymer ligands in buffer containing 0.5 M DTT remained homogeneous and highly fluorescent for at least 6 months. Similarly, the fluorescence images of those QDs in 100% cell growth media (RPMI-1640), shown in Figure 5C, indicate great colloidal stability for at least 2 months, though a slight loss in emission was observed for His−PIMA−PEG−

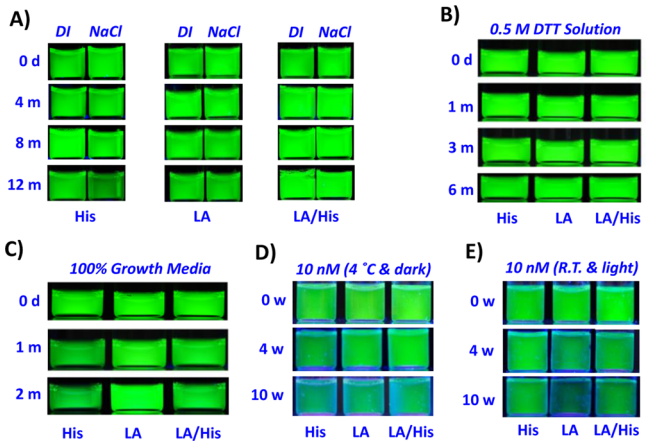

Figure 5. Stability tests applied to three sets of QD dispersions (0.5 μM): (A) in the presence of excess electrolyte (1 M NaCl), (B) diluted in 0.5 M dithiothreitol (DTT) solution, and (C) when mixed with 100% cell growth media. Also shown are the fluorescence images for QDs at 10 nM concentration stored at 4 °C in the dark (D) and under room temperature with white light exposure conditions (E).

QDs. These results are very promising as they indicate the ability of the present coating to impart colloidal stability, while preventing adsorption of proteins and aggregation in biological media. For instance, DTT is a dithiol derivative that can strongly interact with various metal surfaces and effectively compete for binding with an array of small ligands (e.g., DHLA−PEG), promoting aggregation build of metal nanoparticles in buffer media.[37,70] The ability of the newly designed metal-coordinating polymers to impart longer term stability to the QDs in 0.5 M DTT is remarkable and bodes well for use in live cell imaging and sensing.

The final test probed the stability of QD dispersions prepared at very low concentrations (10 nM). The fluorescence images in Figure 5D and E show that all three sets of QD dispersions stayed fluorescent and homogeneous for at least 10 weeks when stored at 4 °C, albeit with a slight decrease in the solution brightness. These dispersions also exhibited great colloidal stability when stored under ambient conditions (room temperature with light exposure) for 10 weeks. Nonetheless, we found that QDs ligated with LA−PIMA−PEG exhibited a slightly higher reduction in the solution brightness compared to the other two samples, a property attributed to potential photo-oxidation of the thiol groups in the ligands.

Overall, the above data confirm the benefits of combining multiple lipoic acid and imidazole groups along with several PEG moieties within the same amphiphilic ligand to improve the colloidal stability of the resulting nanocrystals. Indeed, combining LA and imidazole in the same macromolecule greatly improves the ligand-to-QD binding while maintaining high fluorescence signal in buffer media compared to ligands (polymeric or molecular scale) presenting thiols or imidazoles only anchors. For instance, the fluorescence of His−PIMA−PEG−QDs and LA−PIMA−PEG−QDs exhibited reduction in the PL emission at pH 3, and/or in growth media and ambient conditions. In comparison, dispersions of LA/His−PIMA−PEG−QDs performed better across the various conditions tested. Our data also indicate that QDs capped with $His_{50\%}$−PIMA−$PEG_{50\%}$ exhibit great colloidal stability and high fluorescence at pH 5 (acidic conditions), even though the pK_a of imidazole is ∼6. The ligands with lower imidazole coordinating groups (e.g., $His_{30\%}$−PIMA−$PEG_{70\%}$−QDs)

DOI: 10.1021/jacs.5b00671
J. Am. Chem. Soc. 2015, 137, 5438−5451

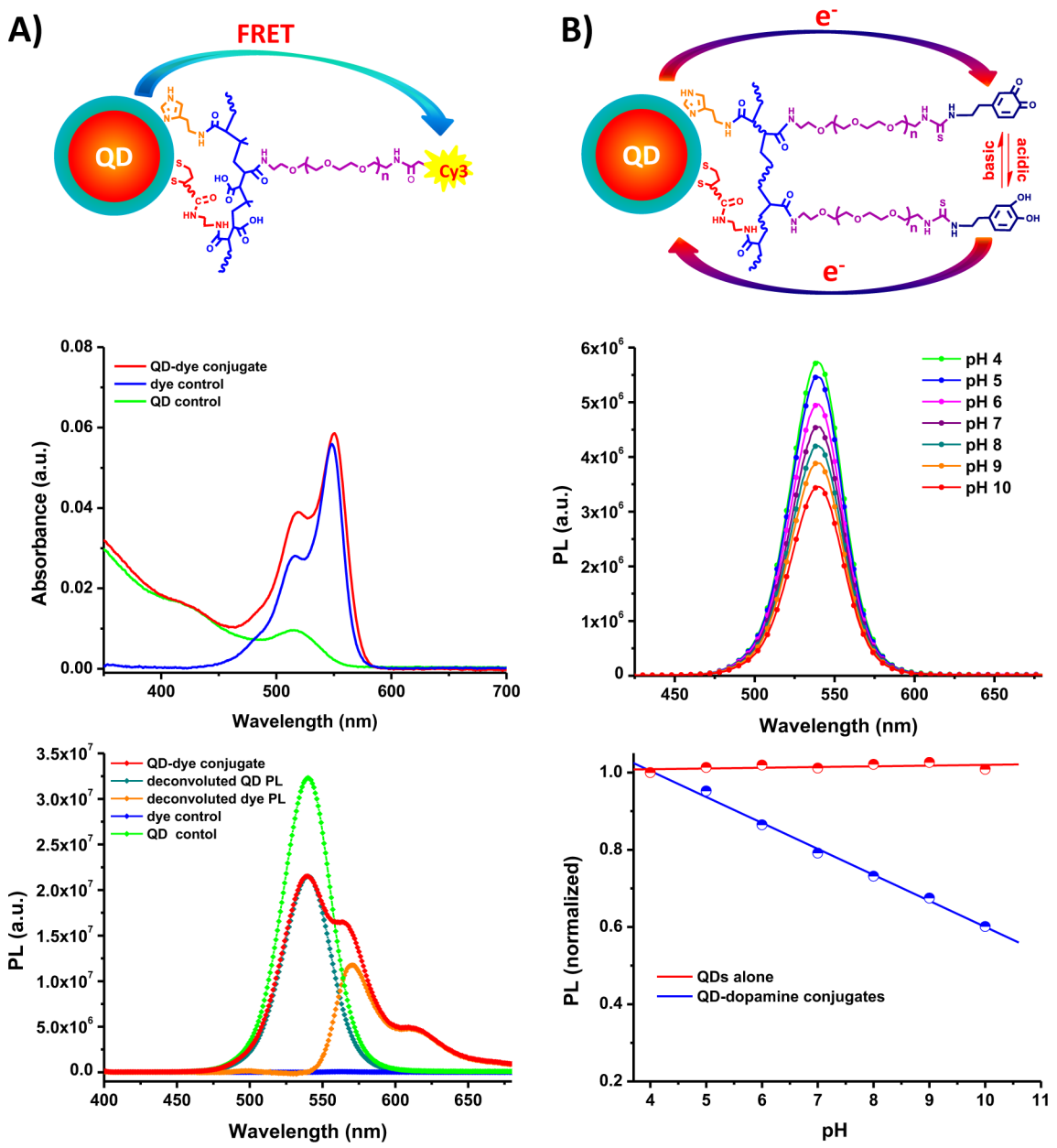

Figure 6. (A) (top) Schematic representation of the covalent conjugation of sulfo-Cy3 NHS-ester dye to amine-functionalized QDs. (middle) Absorption spectra collected from purified QD–dye conjugates (red), pure QDs (green), and pure dye (blue) in water. (bottom) Composite emission spectrum of QD–dye conjugates (red), together with the deconvoluted contributions of the QDs (dark green) and dye (orange). The fluorescence spectra were generated using 350-nm excitation. (B) (top) Schematics of the assembly of dopamine-ITC onto amine-functionalized QDs via isothiourea bond. Steady-state fluorescence spectra collected from solutions of QD–dopamine conjugates in buffers ranging from pH 4 to 10 (middle), together with the corresponding integrated PL intensities normalized with respect to the value at pH 4 (bottom). The PL intensity of QDs alone was insensitive to pH changing (red).

provide weaker colloidal stability at pH 5 (see SI Figure S10), consistent with a previous report.[44] These findings combined clearly reflect the benefits of high coordination afforded by the polymer ligand compared to those presenting lower coordination numbers.

Further Functionalization of the Polymer-Coated QDs. Introduction of reactive groups into the polymer structure allows further coupling to specific molecules (e.g., dyes and peptides). As such we have explored activation of amines on QDs photoligated with LA/His–PIMA–PEG–NH_2 with two distinct functionalities, along with activation of carboxylic groups available on QDs ligated with LA/His–PIMA–PEG–OCH_3 as follows: (1) coupling to Cy3 dye to test energy transfer interactions; (2) coupling to the neurotransmitter dopamine to provide a pH-sensitive fluorescent platform where emission is controlled by pH-dependent charge transfer interactions, and (3) EDC/NHS-driven modification of the carboxylic groups along the polymer backbone, freed during the ligand synthesis, with cell penetrating peptides (CPP) to form QD–CPP conjugates and promote intracellular uptake and imaging.

1. Covalent Conjugation to FRET Dyes. Amine-functionalized nanocrystals (QDs photoligated with LA/His–PIMA–PEG–amine) were reacted with NHS-ester-modified sulfo-Cy3

DOI: 10.1021/jacs.5b00671
J. Am. Chem. Soc. 2015, 137, 5438–5451

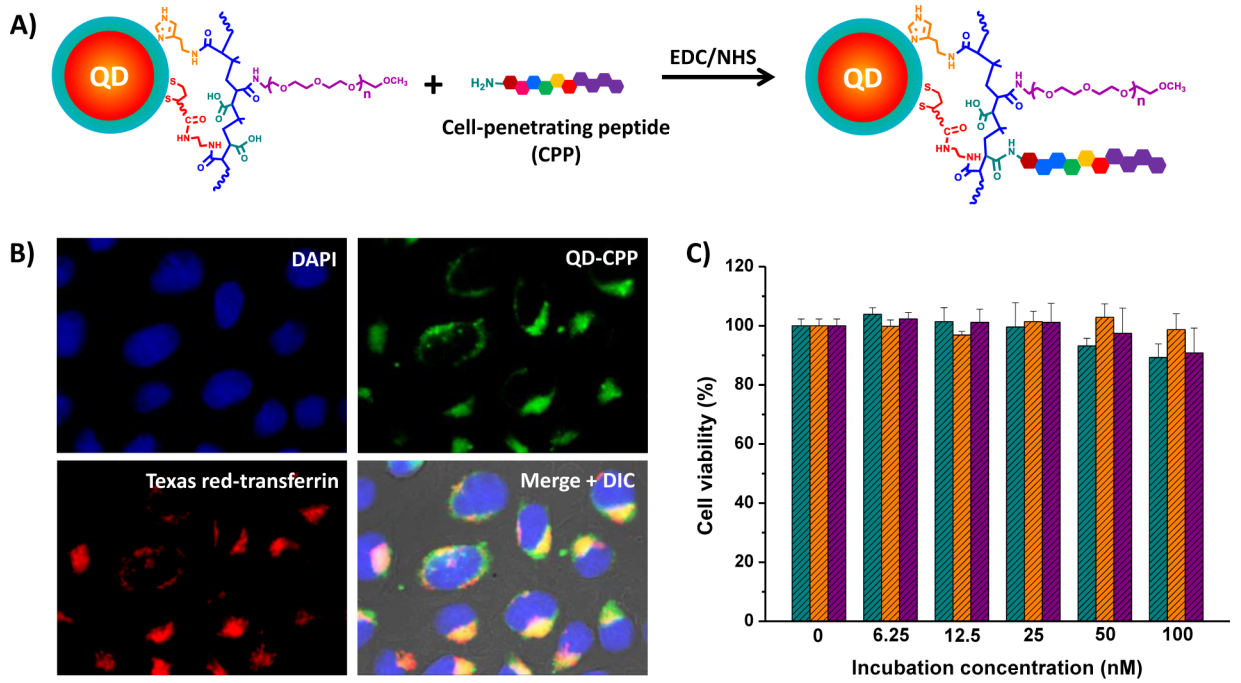

Figure 7. (A) Schematic representation of the QD−CPP conjugate assembled via EDC/NHS coupling. The average number of CPP per QD is ∼10, assuming 100% reaction efficiency using CPP:QD molar ratio of 10:1. (B) Representative epifluorescence images of HeLa cells incubated with QD−CPP conjugates at 200 nM for 1 h. Images correspond to the DAPI emission, QD emission at 537 nm, Texas Red-transferrin emission (as an endosome-specific marker), and the merged images. (C) MTT viability tests of HeLa cells incubated for 24 h with varying concentrations of QDs ligated with the three sets of polymers: LA−PIMA−PEG (dark cyan), His−PIMA−PEG (orange), and LA/His−PIMA−PEG (purple). QDs emitting at 537 nm were used.

following conventional protocols (see schematics in Figure 6).[58] After removal of excess unreacted dye and byproducts, the absorption and PL spectra were collected. The data shown in Figure 6A indicate that the absorption spectrum collected from the conjugates is a composite of QD and Cy3 dye contributions. Furthermore, deconvolution of the composite photoluminescence spectrum (using 350-nm excitation) shows a sizable decrease in the QD fluorescence along with an increase in the dye contribution; in comparison a negligible direct excitation contribution is measured from a control Cy3 alone (blue curve). Following deconvolution of the absorption spectra of the conjugates and using the extinction coefficients of the dye and QD, we estimate that the average number of conjugated Cy3 per QD is equal to 2.8 (∼3). The FRET efficiency calculated using the relation $E = 1 - F_{DA}/F_D$, where F_{DA} and F_D designate the PL intensity measured for QD-Cy3 conjugates and QDs alone, is 33.4%. Comparison to the FRET efficiency extracted from the Förster dipole−dipole model using the experimental spectral overlap integral indicates that the center-to-center separation distance is about 61 Å, which further proves that the polymer coating developed here provides a rather compact coating of the QD. Additional details on the FRET analysis are provided in SI Table S1.

2. Coupling to Dopamine Yields a pH-Controlled QD Photoluminescence. We further tested the reactivity of the QDs ligated with LA/His−PIMA−PEG−NH_2 by reacting them with dopamine-ITC, which yields QD−dopamine conjugates via a covalent isothiourea bond.[24] After removal of the excess unreacted dopamine-ITC, we tracked the changes in the PL collected from QD−dopamine conjugates using steady-state and time-resolved fluorescence measurements when the pH of the buffer was progressively switched from acidic to alkaline. Figure 6B shows that the PL spectra collected from dispersions of these conjugates change with increasing pH, as reported for other QD−dopamine conjugates.[24] The above PL loss is coupled with a progressive shortening in the QD PL lifetime when the solution pH is changed (as shown in SI Figure S11). Cumulative plots for the relative changes in PL with the solution pH show a decrease in the PL intensity with increasing solution pH. In comparison, there are no measurable changes in the PL for control dispersions made of polymer-coated QDs but without coupled dopamine. The progressive loss in QD PL with increasing pH is attributed to the pH-dependent chemical transformation of dopamine: namely a decrease in the oxidation potential of the catechol (reduced form) combined with increased concentration of quinone (oxidized form) when the pH of the buffer is increased, as schematically illustrated in Figure 6B.[24] Both transformations promote a pH-dependent enhancement in the charge transfer interactions for the QD−dopamine conjugates, manifesting in a progressive and pronounced quenching of the QD PL with increasing pH.

3. Intracellular Uptake of QD−CPP Conjugates and Cytotoxicity Tests. Here we started with LA/His−PIMA−PEG−OCH_3-capped QDs which were further coupled to cell-penetrating peptides (CPP) via EDC/NHS chemistry, as illustrated in Figure 7A. The carboxylic acid groups freed along the PIMA backbone were activated with EDC/NHS, and then amine-terminated CPP were added to promote carboxyl-to-amine cross-linking. Following purification using a PD10 column, the conjugates were tested for their ability to promote intracellular uptake. We estimated that there were ∼10 CPP per QD−conjugate, assuming 100% reaction efficiency when starting with a CPP:QD molar ratio of 10:1. Figure 7B shows a representative set of fluorescence images collected for HeLa

DOI: 10.1021/jacs.5b00671
J. Am. Chem. Soc. 2015, 137, 5438−5451

cells incubated with QD−CPP conjugates at 200 nM for 1 h. The images show that the QD green signal is observed only in cells incubated with the QD−CPP conjugates, but no intracellular QD fluorescence is detected for the cells incubated with the same concentration of unconjugated QDs, indicating that CPP promotes intracellular delivery of the conjugates; images of cells incubated with QDs only are provided in SI Figure S12. Furthermore, the green fluorescence is distributed within the perinuclear region of the cells and is mostly colocalized with the distribution of endo/lysosomal compartments (counterstained with Texas Red-labeled transferrin). These results provide strong evidence that conjugating CPP to QDs promotes cellular internalization, presumably via endocytotic uptake.[71]

We also assessed the cytotoxicity of QDs ligated with LA−PIMA−PEG, His−PIMA−PEG, and LA/His−PIMA−PEG to HeLa cells following 24-h incubation using MTT assay, as shown in Figure 7C. The data show that the viability of cells incubated with QDs coated with these three sets of ligands essentially remained at 100% throughout the conjugate concentrations used (0−100 nM). These findings indicate that, overall, QDs capped with the polymer ligands containing PEG moieties induce minimal to no toxicity to cell cultures.

CONCLUSION

We have designed and optimized a set of multicoordinating amphiphilic polymer ligands ideally suited for surface-functionalizing QDs. The ligand design relies on the specific and highly efficient nucleophilic addition between poly(isobutylene-*alt*-maleic anhydride) and a set of amine-modified target functions. Using this synthetic platform, we were able to introduce large but controllable numbers of anchoring, hydrophilic, and reactive groups onto a PIMA chain. In particular, we have combined two distinct metal-coordinating groups, dihydrolipoic acid and imidazole, along with PEG moieties within the same ligand. This combination provides additional flexibility and addresses issues of quenching and potential oxidation of thiol-based ligands and weak binding affinity of imidazole-based ligands. We further combine this ligand design with a mild photoligation strategy to promote the in situ ligand exchange and phase transfer of hydrophobic QDs to aqueous media under borohydride-free conditions.

This strategy yields compact polymer-capped QDs that exhibit great colloidal stability over a broad range of conditions, such as pH 3−13, in high ionic strength buffer, in the presence of dithiothreitol, and in cell growth media. Furthermore, hydrophilic dispersions of polymer-coated QDs at very low concentration (10 nM) that are colloidally stable under ambient conditions (room temperature and light exposure) have been prepared and tested. This result is promising for fluorescent labeling in biology, such as intracellular imaging and sensing, where very small reagent concentrations are often required. We also show that these QDs can be functionalized with reactive dye, redox-active dopamine, and cell-penetrating peptide using conventional coupling strategies. Furthermore, MTT viability assays indicate that these polymer-ligated QDs elicit little to no cytotoxicity. Finally, we would like to stress that the present multifunctional polymer platform is ideally adapted for orthogonal chemistry, as one can easily introduce at least two different reactive groups (e.g., carboxy-plus-amine, carboxy-plus-azide, carboxy-plus-amine and biotin) during the nucelophilic addition step and without requiring addition post synthesis steps. In addition, the present ligand design can be easily adapted to a variety of other inorganic nanocrystals, such as iron oxide and metal nanoparticles, by replacing the metal chelating groups.[59,67]

EXPERIMENTAL SECTION

We focus on the synthesis of two representative ligands: LA/His−PIMA−PEG and LA/HIS−PIMA−PEG−NH_2. Additional details on the syntheses of other ligands based on the same PIMA platform are provided in the Supporting Information.

Synthesis of LA/His−PIMA−PEG (30% His, 20% LA, and 50% PEG). Poly(isobutylene-*alt*-maleic anhydride) (0.385 g, 2.5 mmol monomer units) was dissolved in 10 mL of dry DMF using a 50-mL three-necked round-bottomed flask equipped with an addition funnel and a magnetic stirring bar. The solution was purged with nitrogen and then heated to 40 °C. Separately, two vials, one containing a mixture of LA−NH_2 (0.124 g, 0.5 mmol) and H_2N−PEG−OMe (0.47 g, 0.625 mmol) dissolved in 2 mL of DMF and the other containing histamine (0.0834 g, 0.75 mmol) and H_2N−PEG−OMe (0.47 g, 0.625 mmol) in 2 mL of DMF were prepared. The content of each vial was loaded separately into the addition funnel and added dropwise to the PIMA solution. When the addition was complete, the reaction mixture was left stirring overnight at 40 °C. The solvent was removed under vacuum and then chloroform (3 mL) was added. The solution was loaded onto a silica column and the compound was purified with chloroform as the eluent to collect the final product (as a yellow gel), with a yield ∼91%.

Synthesis of LA/His−PIMA−PEG−R (30% His, 20% LA, 50% PEG, and 5% amine). PIMA (0.385 g, 2.5 mmol monomer units) dissolved in 10 mL of dry DMF was added into a 50-mL three-necked round-bottomed flask equipped with an addition funnel; the solution was heated to 40 °C while stirring. To the flask, 2 mL of DMF solution containing LA−NH_2 (0.124 g, 0.5 mmol) and H_2N−PEG−OMe (0.28 g, 0.375 mmol) was added dropwise through the addition funnel. Following that, 2 mL of DMF solution containing histamine (0.0834 g, 0.75 mmol) and H_2N−PEG−OMe (0.28 g, 0.375 mmol) was added also dropwise, and the mixture was left stirring for 1 h. Then, H_2N−PEG−NH_2 (0.075 g, 0.125 mmol) and H_2N−PEG−OMe (0.28 g, 0.375 mmol) dissolved in 2 mL of DMF were finally added to the flask. When the addition was complete, the reaction mixture was left stirring at 40 °C overnight, and then the solvent was removed under vacuum. The ligand was further purified onto a silica column and chloroform was used as the eluent to collect the final product, with a yield ∼85%.

Growth of CdSe−ZnS Core−Shell Quantum Dots. The QD samples were prepared in two reaction steps via reduction of organometallic precursors at high temperature in a hot coordinating solvent mixture. The CdSe core was gown first via reduction of cadmium and selenium precursors at ∼300−350 °C using a coordinating solvent mixture made of trioctyl phosphine (TOP), trioctyl phosphine oxide (TOPO), and alkylamines along with a small fraction of hexylphosphonic acid; the CdSe nanocrystal size was controlled via small adjustments in the precursor concentrations and annealing temperature.[2,3,7] The CdSe core was overcoated with a shell made of a few monolayers (here ∼5−6) of ZnS using zinc and sulfur precursors, but the procedure was carried out at lower temperature (150−180 °C).[8−10] All QDs were prepared to have similar overcoating ZnS layer; the overall core−shell size difference is primarily due to variation in the core radius.

Ligand Exchange of Quantum Dots with His−PIMA−PEG. Hydrophobic QDs (150 μL; 26.7 μM) were precipitated using ethanol (or a mixture of methanol and butanol) and redispersed in 100 μL of THF. Then 25 mg of His−PIMA−PEG dissolved in 150 μL of THF was added to the QD solution; a homogeneous solution resulted. The vial was sealed with a rubber septum, and the atmosphere was switched to nitrogen by applying 2−3 rounds of mild vacuum, followed by purging with nitrogen. The solution was heated to 40 °C, and then left stirring for 2 h. The QD samples were precipitated by adding excess (∼5 mL) hexane and centrifuged at 3700 rpm for 5 min yielding a yellow pellet. The clear supernatant was discarded, and the

DOI: 10.1021/jacs.5b00671
J. Am. Chem. Soc. 2015, 137, 5438−5451

pellet was redissolved in 200 μL of THF, followed by another round of precipitation using excess hexane. The precipitate was dried under vacuum, then dispersed in DI water. After sonication, the clear aqueous dispersion was filtered through a 0.45-μm disposable syringe filter, and the excess free ligands were removed by applying 3−4 rounds of concentration/dilution using a centrifugal filtration device (Millipore, MW cutoff = 50 kDa). This afforded clear QD solution with final volume of ∼500 μL and a concentration of ∼7−8 μM, as estimated from the absorption data and the extinction coefficient of the QD material.[72]

Remark. The above procedure can also be applied to His/LA−PIMA−PEG ligand. This yields hydrophilic QDs where the imidazole groups drive the coordination onto the QD surfaces, while the lipoic acids (in the form of dithiolanes) stay free and laterally exposed for potential additional transformation targeting the dithiolane ring (see Figure 2).

Photoligation of Quantum Dots with LA−PIMA−PEG. The phase transfer of the QDs with LA-containing ligands was carried using a photoligation strategy we have recently developed.[60] Here, cap exchange of the LA groups is photochemically induced under borohydride-free conditions. This procedure was carried out by UV photoirradiation of the hydrophobic QDs mixed with LA-containing polymer(s). Briefly, QDs (26.7 μM, 150 μL) were precipitated using ethanol and redispersed in 100 μL of THF. Then 200 μL of THF containing LA−PIMA−PEG (25 mg) was mixed with the QD solution, followed by the addition of 30 μL of tetramethylammonium hydroxide (∼5 mM) predissolved in methanol. The vial was sealed with a rubber septum, and the atmosphere was switched to nitrogen by applying 2−3 rounds of mild vacuum followed by flushing with nitrogen. The vial was then placed inside the UV photoreactor and irradiated for 20 min (at 350 nm, 4.5 mW/cm^2) with stirring. Hexane was then added to precipitate out the QDs. The sample was centrifuged at 3700 rpm for 5 min, and the precipitated pellet was redispersed in 200 μL of THF. Another round of precipitation with excess hexane was applied, and the resulting QD pellet was dried under vacuum and dispersed in DI water. The aqueous dispersion was then filtered through a 0.45-μm syringe filter and purified by applying 3−4 rounds of concentration/dilution using a membrane filtration device (Amicon Ultra 50 kDa from Millipore) to remove excess ligands.

Photomediated Ligand Exchange with LA/His−PIMA−PEG. QDs (26.7 μM, 150 μL) were precipitated using ethanol and dispersed in 100 μL of THF. This solution was mixed with 200 μL of THF containing 25 mg of LA/His−PIMA−PEG. The vial was sealed with a rubber septum, purged with nitrogen, and the solution was stirred for 2 h at 40 °C. A methanol solution of tetramethylammonium hydroxide (5 mM, 30 μL) was added, followed by UV irradiation (using the UV reaction) for 10 min. Two rounds of precipitation with excess hexanes were applied and the QD pellet was dried under vacuum and dispersed in DI water. The aqueous dispersion was then filtered through a syringe filter and further purified by applying 3−4 rounds of concentration/dilution (MW cutoff = 50 kDa). Alternatively, the phase transfer of QDs to DI water can be carried out before performing the UV irradiation. Briefly, following precipitation of the native QDs with ethanol and centrifugation, the pellet of TOP/TOPO QDs was dispersed in 100 μL of THF and mixed with 25 mg of LA/His−PIMA−PEG predissolved in 200 μL of THF. The mixture was left stirring for 2 h and precipitated with excess hexane. The precipitated QD pellet was dried under vacuum and dispersed in 200 μL of DI water. An aqueous solution of tetramethylammonium hydroxide (5 mM, 30 μL) was added followed by UV irradiation for 10 min. The QDs were filtered through a 0.45-μm syringe filter, and purified by applying 3−4 rounds of concentration/dilution using a membrane filtration device as done above.

NMR Characterization of the Hydrophilic QDs. We used pulsed-field gradient-based water suppression ^{1}H NMR to collect our spectra. The solvent was switched from hydrogenated DI water to deuterated water by applying two rounds of concentration/dilution using 2 mL of D_2O each. The final volume of the dispersion in D_2O used to collect the spectra was adjusted to 450 μL. For instance, the spectra shown in Figure 3 were collected using a dispersion of LA/His−PIMA−PEG QDs at a concentration of 18 μM and averaged over 500 scans. The sample used for the ligand counting experiments was prepared following the same protocol, except that 0.6 μL of pyridine (7.45 μmol) was added to provide a standard/reference to which the signature of the polymer-capped QDs was compared. We also characterized the filtrate collected in the bottom of the device using ^{1}H NMR spectroscopy. We found no sign of free ligands in the filtrates, as the purification steps were able to reduce the concentration of excess ligands to below the detection limit of the instrument.

Conjugation of Amine QDs to Cy3 Dye. Green-emitting QDs ligand-exchanged with LA/His−PIMA−PEG−NH_2 were reacted with sulfo-Cy3 NHS ester to provide QD−dye conjugates. Briefly, 117 μL of amine-functionalized QDs (8.52 μM) was dispersed in 373 μL of phosphate buffer (50 mM, pH = 8.0), and then 15 equiv of activated sulfo-Cy3 NHS ester dye dissolved in DMSO (at 1.5 mM in 10 μL) was added. The reaction mixture was left to proceed for ∼1.5 h at room temperature, then the QD−dye conjugates were separated from unbound dye and NHS byproduct via size-exclusion chromatography (using PD 10 column); the first eluted fraction of QD−dye conjugates was characterized using absorption and fluorescence measurements.

Assembly of the QD−Dopamine Conjugates. To a vial containing 1 mL of DI water, we added 94 μL of amine-functionalized QDs (concentrations = 8.52 μM) and 11 μL of dopamine-isothiocyanate (dopamine-ITC) predissolved in DMSO (0.5 mg/mL). The dopamine-ITC was prepared in our laboratory following previous protocols.[24] The mixture was stirred for 3−3.5 h in the dark, followed by removal of excess free/unreacted dopamine by applying one round of concentration/dilution using a membrane filtration device (MW cutoff: 50 kDa, Millipore); DI water was then added to the purified materials to provide a stock dispersion of QD-conjugates with a concentration of ∼0.8 μM. Aliquots (40 μL) of this stock dispersion were then mixed with 960 μL of phosphate buffer (10 mM) at the desired pH (e.g., pH 4−10). These conjugates were then used to collect the steady-state florescence and time-resolved fluorescence data.

Assembly of the QD−CPP Conjugates. To prepare QD−CPP conjugates, the carboxylic groups (freed during the addition reaction) available on the surface of QDs ligated with LA/His−PIMA−PEG were targeted for coupling with amine-terminated CPP via EDC/NHS reaction.[51] Briefly, 100 μL of QDs (9.3 μM) was dispersed in 400 μL of phosphate buffer (50 mM, pH = 6.5), and then 50 equiv of NHS (8.5 mM, 6 μL) and EDC (5 mM, 10 μL) in aqueous solution were added. The reaction was left to proceed for ∼1.5 h at room temperature, then the excess EDC and NHS were removed using one round of concentration/dilution with DI water through a membrane filtration device (MW cutoff: 50 kDa, Millipore). The purified QD-NHS esters were added to 400 μL of phosphate buffer (50 mM, pH = 8.0) containing ∼10-fold excess of CPP (4.6 mM, 2 μL) with respect to QDs. The mixture was left to react at room temperature for 2 h. The conjugates were separated from unbound CPP and NHS byproduct via size-exclusion chromatography (using PD 10 column); the first eluted fraction containing the QD−CPP conjugates was used for the cellular uptake experiments.

Fluorescence Imaging of Live Cells. HeLa cell cultures (human cervix carcinoma cell line, provided by the FSU cell culture facility) were grown at 37 °C in a humidified 5% CO_2 atmosphere at 37 °C, as a monolayer in a complete growth medium (Dulbecco's Modified Eagle's Medium, DMEM, Cellgro), supplemented with 10% (v/v) fetal bovine serum (Gibco), 4.5 g/L glucose, L-glutamine, sodium pyruvate, 1% (v/v) antibiotic-antimycotic 100x (Gibco), and 1% (v/v) nonessential amino-acid solution 100x (Sigma). 8×10^4 of the above cells were first seeded onto 12-mm circle microcover glasses (VWR) for 24-well microplates (CellStar, VWR), and the plates were placed in an incubator overnight to allow for cell attachment. After 24 h, the cells were mixed with the QD−CPP conjugates (at a concentration of 200 nM) and Texas red-labeled transferrin (at a concentration of ∼0.5 μM). The cells were left to incubate for 1 h. After incubation, the cells were washed with PBS buffer two times, fixed with 3.7% paraformaldehyde, and stained with 4,6-diamino-2-

DOI: 10.1021/jacs.5b00671
J. Am. Chem. Soc. 2015, 137, 5438−5451

phenylindole (Prolong Antifade mounting media with DAPI nuclear staining, Invitrogen). Control experiments were carried out by incubating the cells with unconjugated QDs (without CPP). The fluorescence images were acquired using an Inverted Research Nikon Eclipse Ti Microscope equipped with a color CoolSNAP HQ2 CCD camera. Excitation of the sample was provided by a Xe lamp, while the fluorescence images were collected using a 60× objective (Nikon) and a set of filter cubes (Chroma Technology (Rockingham, VT). The DAPI fluorescence was detected using a DAPI cube (with 340−380 nm excitation and 435−485 nm emission line). The QD fluorescence signal was detected using a GFP/EGFP cube (with 465−495 nm excitation and 515−555 nm emission line). The Texas Red-transferrin florescence was detected using a TEXAS RED HYQ cube (with 532−587 nm excitation and 608−683 nm emission line).

Viability Assays. The viability of HeLa cells incubated with QDs capped with LA−PIMA−PEG, His−PIMA−PEG, and LA/His−PIMA−PEG ligands at concentrations of 0, 6.25, 12.5, 25, 50, and 100 nM was tested using MTT (3-(4,5-dimethylthiazol-2-yl)-2,5-diphenyltetrazolium bromide) assay. MTT assay is a colorimetric test based on the cellular reduction of MTT (Sigma-Aldrich Chemical) by the mitochondrial dehydrogenase of viable cells, forming a blue formazan product which can be measured spectrophotometrically. MTT solution was prepared at 5 mg/mL in PBS 1X and then diluted 1:5 in medium without serum or Phenol Red. Cells were first seeded into 96-well microplates (2×10^4 cells/200 μL/well), and the microplates were placed in an incubator overnight to allow adherence. Dispersions of QDs were then applied directly to the wells using a multichannel pipet (in triplicate), and the cultures were incubated for 24 h at 37 °C. After incubation, the media was removed, the cells were washed twice with PBS 1X, then 200 μL of the MTT solution (0.2 mg/mL) was added to each well and left to incubate for 4 h at 37 °C. The MTT solution was removed, and 100 μL of 100% DMSO was added to each well to solubilize the MTT-formazan product. Absorbance at 560 nm was measured using a plate reader (the Infinite M1000 PRO from TECAN). The cell viability obtained from the absorbance measurements was expressed as a fraction of viable cells and normalized to that of cells that were not exposed to the QDs.

■ ASSOCIATED CONTENT

Supporting Information

Materials, instrumentation, additional experimental details, ^{1}H NMR characterization of the polymer ligands, UV absorption spectra of ligands, optical characterization of LA−PIMA−PEG-capped QDs and His−PIMA−PEG-capped QDs, ^{1}H NMR spectrum of TOP/TOPO/HPA-capped QDs, ^{1}H NMR spectrum of LA/His−PIMA−PEG-capped QDs calibrated with pyridine, colloidal stability test of $His_{30\%}$−PIMA−$PEG_{70\%}$-capped QDs, FRET analysis, time-resolved PL decays of QD−dopamine conjugate, and control experiment of cellular uptake of QDs alone. This material is available free of charge via the Internet at http://pubs.acs.org.

■ AUTHOR INFORMATION

Corresponding Author

*mattoussi@chem.fsu.edu

Notes

The authors declare no competing financial interest.

■ ACKNOWLEDGMENTS

We thank FSU and the National Science Foundation for financial support (NSF-CHE 1058957).

■ REFERENCES

(1) Alivisatos, A. P. *Science* **1996**, *271*, 933.
(2) Murray, C. B.; Kagan, C. R.; Bawendi, M. G. *Annu. Rev. Mater. Sci.* **2000**, *30*, 545.
(3) Peng, Z. A.; Peng, X. G. *J. Am. Chem. Soc.* **2001**, *123*, 183.
(4) Rogach, A. L.; Talapin, D. V.; Shevchenko, E. V.; Kornowski, A.; Haase, M.; Weller, H. *Adv. Funct. Mater.* **2002**, *12*, 653.
(5) Klimov, V. I., Ed. *Nanocrystal Quantum Dots*, 2nd ed.; CRC Press: Boca Raton, FL, 2010.
(6) Talapin, D. V.; Lee, J. S.; Kovalenko, M. V.; Shevchenko, E. V. *Chem. Rev.* **2010**, *110*, 389.
(7) Murray, C. B.; Norris, D. J.; Bawendi, M. G. *J. Am. Chem. Soc.* **1993**, *115*, 8706.
(8) Hines, M. A.; Guyot-Sionnest, P. *J. Phys. Chem.* **1996**, *100*, 468.
(9) Dabbousi, B. O.; RodriguezViejo, J.; Mikulec, F. V.; Heine, J. R.; Mattoussi, H.; Ober, R.; Jensen, K. F.; Bawendi, M. G. *J. Phys. Chem. B* **1997**, *101*, 9463.
(10) Reiss, P.; Bleuse, J.; Pron, A. *Nano Lett.* **2002**, *2*, 781.
(11) Medintz, I. L.; Uyeda, H. T.; Goldman, E. R.; Mattoussi, H. *Nat. Mater.* **2005**, *4*, 435.
(12) Resch-Genger, U.; Grabolle, M.; Cavaliere-Jaricot, S.; Nitschke, R.; Nann, T. *Nat. Methods* **2008**, *5*, 763.
(13) Bruchez, M.; Moronne, M.; Gin, P.; Weiss, S.; Alivisatos, A. P. *Science* **1998**, *281*, 2013.
(14) Chan, W. C. W.; Nie, S. M. *Science* **1998**, *281*, 2016.
(15) Wu, X. Y.; Liu, H. J.; Liu, J. Q.; Haley, K. N.; Treadway, J. A.; Larson, J. P.; Ge, N. F.; Peale, F.; Bruchez, M. P. *Nat. Biotechnol.* **2003**, *21*, 452.
(16) Dahan, M.; Levi, S.; Luccardini, C.; Rostaing, P.; Riveau, B.; Triller, A. *Science* **2003**, *302*, 442.
(17) Gao, X. H.; Cui, Y. Y.; Levenson, R. M.; Chung, L. W. K.; Nie, S. M. *Nat. Biotechnol.* **2004**, *22*, 969.
(18) Michalet, X.; Pinaud, F. F.; Bentolila, L. A.; Tsay, J. M.; Doose, S.; Li, J. J.; Sundaresan, G.; Wu, A. M.; Gambhir, S. S.; Weiss, S. *Science* **2005**, *307*, 538.
(19) Snee, P. T.; Somers, R. C.; Nair, G.; Zimmer, J. P.; Bawendi, M. G.; Nocera, D. G. *J. Am. Chem. Soc.* **2006**, *128*, 13320.
(20) Gill, R.; Zayats, M.; Willner, I. *Angew. Chem. Int. Ed.* **2008**, *47*, 7602.
(21) Yildiz, I.; Deniz, E.; Raymo, F. M. *Chem. Soc. Rev.* **2009**, *38*, 1859.
(22) Zrazhevskiy, P.; Sena, M.; Gao, X. H. *Chem. Soc. Rev.* **2010**, *39*, 4326.
(23) Mattoussi, H.; Palui, G.; Na, H. B. *Adv. Drug Deliver Rev.* **2012**, *64*, 138.
(24) Ji, X.; Palui, G.; Avellini, T.; Na, H. B.; Yi, C. Y.; Knappenberger, K. L.; Mattoussi, H. *J. Am. Chem. Soc.* **2012**, *134*, 6006.
(25) Freeman, R.; Willner, I. *Chem. Soc. Rev.* **2012**, *41*, 4067.
(26) Kay, E. R.; Lee, J.; Nocera, D. G.; Bawendi, M. G. *Angew. Chem., Int. Ed.* **2013**, *52*, 1165.
(27) Probst, C. E.; Zrazhevskiy, P.; Bagalkot, V.; Gao, X. H. *Adv. Drug Delivery Rev.* **2013**, *65*, 703.
(28) Zhang, F.; Lees, E.; Amin, F.; Gil, P. R.; Yang, F.; Mulvaney, P.; Parak, W. J. *Small* **2011**, *7*, 3113.
(29) Chou, L. Y. T.; Ming, K.; Chan, W. C. W. *Chem. Soc. Rev.* **2011**, *40*, 233.
(30) Sapsford, K. E.; Algar, W. R.; Berti, L.; Gemmill, K. B.; Casey, B. J.; Oh, E.; Stewart, M. H.; Medintz, I. L. *Chem. Rev.* **2013**, *113*, 1904.
(31) Nam, J.; Won, N.; Bang, J.; Jin, H.; Park, J.; Jung, S.; Jung, S.; Park, Y.; Kim, S. *Adv. Drug Delivery Rev.* **2013**, *65*, 622.
(32) Mout, R.; Moyano, D. F.; Rana, S.; Rotello, V. M. *Chem. Soc. Rev.* **2012**, *41*, 2539.
(33) Susumu, K.; Uyeda, H. T.; Medintz, I. L.; Pons, T.; Delehanty, J. B.; Mattoussi, H. *J. Am. Chem. Soc.* **2007**, *129*, 13987.
(34) Zhan, N.; Palui, G.; Safi, M.; Ji, X.; Mattoussi, H. *J. Am. Chem. Soc.* **2013**, *135*, 13786.
(35) Palui, G.; Na, H. B.; Mattoussi, H. *Langmuir* **2012**, *28*, 2761.
(36) Liu, W.; Howarth, M.; Greytak, A. B.; Zheng, Y.; Nocera, D. G.; Ting, A. Y.; Bawendi, M. G. *J. Am. Chem. Soc.* **2008**, *130*, 1274.
(37) Stewart, M. H.; Susumu, K.; Mei, B. C.; Medintz, I. L.; Delehanty, J. B.; Blanco-Canosa, J. B.; Dawson, P. E.; Mattoussi, H. *J. Am. Chem. Soc.* **2010**, *132*, 9804.

DOI: 10.1021/jacs.5b00671
J. Am. Chem. Soc. 2015, 137, 5438−5451

(38) Giovanelli, E.; Muro, E.; Sitbon, G.; Hanafi, M.; Pons, T.; Dubertret, B.; Lequeux, N. *Langmuir* **2012**, *28*, 15177.
(39) Yildiz, I.; McCaughan, B.; Cruickshank, S. F.; Callan, J. F.; Raymo, F. M. *Langmuir* **2009**, *25*, 7090.
(40) Zhu, Z. J.; Yeh, Y. C.; Tang, R.; Yan, B.; Tamayo, J.; Vachet, R. W.; Rotello, V. M. *Nat. Chem.* **2011**, *3*, 963.
(41) Bullen, C.; Mulvaney, P. *Langmuir* **2006**, *22*, 3007.
(42) Liu, W. H.; Greytak, A. B.; Lee, J.; Wong, C. R.; Park, J.; Marshall, L. F.; Jiang, W.; Curtin, P. N.; Ting, A. Y.; Nocera, D. G.; Fukumura, D.; Jain, R. K.; Bawendi, M. G. *J. Am. Chem. Soc.* **2010**, *132*, 472.
(43) Nagaraja, A. T.; Sooresh, A.; Meissner, K. E.; McShane, M. J. *ACS Nano* **2013**, *7*, 6194.
(44) Zhang, P. F.; Liu, S. H.; Gao, D. Y.; Hu, D. H.; Gong, P.; Sheng, Z. H.; Deng, J. H.; Ma, Y. E.; Cai, L. T. *J. Am. Chem. Soc.* **2012**, *134*, 8388.
(45) Han, H. S.; Martin, J. D.; Lee, J.; Harris, D. K.; Fukumura, D.; Jain, R. K.; Bawendi, M. *Angew. Chem. Int. Ed.* **2013**, *52*, 1414.
(46) Viswanath, A.; Shen, Y.; Green, A. N.; Tan, R.; Greytak, A. B.; Benicewicz, B. C. *Macromolecules* **2014**, *47*, 8137.
(47) Susumu, K.; Oh, E.; Delehanty, J. B.; Pinaud, F.; Gemmill, K. B.; Walper, S.; Breger, J.; Schroeder, M. J.; Stewart, M. H.; Jain, V.; Whitaker, C. M.; Huston, A. L.; Medintz, I. L. *Chem. Mater.* **2014**, *26*, 5327.
(48) Medintz, I. L.; Clapp, A. R.; Mattoussi, H.; Goldman, E. R.; Fisher, B.; Mauro, J. M. *Nat. Mater.* **2003**, *2*, 630.
(49) Zylstra, J.; Amey, J.; Miska, N. J.; Pang, L.; Hine, C. R.; Langer, J.; Doyle, R. P.; Maye, M. M. *Langmuir* **2011**, *27*, 4371.
(50) Paiva, T. B.; Tominaga, M.; Paiva, A. C. *J. Med. Chem.* **1970**, *13*, 689.
(51) Hermanson, G. T.*Bioconjugate Techniques*, 3rd ed.; Academic Press, 2013; p 1.
(52) Pellegrino, T.; Manna, L.; Kudera, S.; Liedl, T.; Koktysh, D.; Rogach, A. L.; Keller, S.; Radler, J.; Natile, G.; Parak, W. J. *Nano Lett.* **2004**, *4*, 703.
(53) Yu, W. W.; Chang, E.; Falkner, J. C.; Zhang, J. Y.; Al-Somali, A. M.; Sayes, C. M.; Johns, J.; Drezek, R.; Colvin, V. L. *J. Am. Chem. Soc.* **2007**, *129*, 2871.
(54) Lin, C. A.; Sperling, R. A.; Li, J. K.; Yang, T. Y.; Li, P. Y.; Zanella, M.; Chang, W. H.; Parak, W. J. *Small* **2008**, *4*, 334.
(55) Lees, E. E.; Nguyen, T. L.; Clayton, A. H. A.; Muir, B. W.; Mulvaney, P. *ACS Nano* **2009**, *3*, 2049.
(56) Janczewski, D.; Tomczak, N.; Han, M. Y.; Vancso, G. J. *Nat. Protoc.* **2011**, *6*, 1546.
(57) Diaz, S. A.; Giordano, L.; Jovin, T. M.; Jares-Erijman, E. A. *Nano Lett.* **2012**, *12*, 3537.
(58) Susumu, K.; Mei, B. C.; Mattoussi, H. *Nat. Protoc.* **2009**, *4*, 424.
(59) Wang, W.; Ji, X.; Na, H. B.; Safi, M.; Smith, A.; Palui, G.; Perez, J. M.; Mattoussi, H. *Langmuir* **2014**, *30*, 6197.
(60) Palui, G.; Avellini, T.; Zhan, N.; Pan, F.; Gray, D.; Alabugin, I.; Mattoussi, H. *J. Am. Chem. Soc.* **2012**, *134*, 16370.
(61) Bucher, G.; Lu, C. Y.; Sander, W. *ChemPhysChem* **2005**, *6*, 2607.
(62) Tsay, J. M.; Doose, S.; Pinaud, F.; Weiss, S. *J. Phys. Chem. B* **2005**, *109*, 1669.
(63) Manna, L.; Scher, E. C.; Li, L. S.; Alivisatos, A. P. *J. Am. Chem. Soc.* **2002**, *124*, 7136.
(64) Lee, S. F.; Osborne, M. A. *J. Am. Chem. Soc.* **2007**, *129*, 8936.
(65) Rodríguez-Viejo, J.; Mattoussi, H.; Heine, J. R.; Kuno, M. K.; Michel, J.; Bawendi, M. G.; Jensen, K. F. *J. Appl. Phys.* **2000**, *87*, 8526.
(66) Pons, T.; Uyeda, H. T.; Medintz, I. L.; Mattoussi, H. *J. Phys. Chem. B* **2006**, *110*, 20308.
(67) Wang, W.; Aldeek, F.; Ji, X.; Zeng, B.; Mattoussi, H. *Faraday Discuss.* **2014**, *175*, 137.
(68) Mattoussi, H.; Cumming, A. W.; Murray, C. B.; Bawendi, M. G.; Ober, R. *Phys. Rev. B* **1998**, *58*, 7850.
(69) Oh, E.; Susumu, K.; Blanco-Canosa, J. B.; Medintz, I. L.; Dawson, P. E.; Mattoussi, H. *Small* **2010**, *6*, 1273.
(70) Gravel, E.; Tanguy, C.; Cassette, E.; Pons, T.; Knittel, F.; Bernards, N.; Garofalakis, A.; Duconge, F.; Dubertret, B.; Doris, E. *Chem. Sci.* **2013**, *4*, 411.
(71) Delehanty, J. B.; Bradburne, C. E.; Boeneman, K.; Susumu, K.; Farrell, D.; Mei, B. C.; Blanco-Canosa, J. B.; Dawson, G.; Dawson, P. E.; Mattoussi, H.; Medintz, I. L. *Integr. Biol.* **2010**, *2*, 265.
(72) Leatherdale, C. A.; Woo, W. K.; Mikulec, F. V.; Bawendi, M. G. *J. Phys. Chem. B* **2002**, *106*, 7619.

DOI: 10.1021/jacs.5b00671
J. Am. Chem. Soc. 2015, 137, 5438−5451